



Research Article

Wavelength-dependent DNA Photodamage in a 3-D human Skin Model over the Far-UVC and Germicidal UVC Wavelength Ranges from 215 to 255 nm

David Welch* , Marilena Aquino de Muro, Manuela Buonanno  and David J. Brenner

Center for Radiological Research, Columbia University Irving Medical Center, New York, NY

Received 14 December 2021, accepted 28 January 2022, DOI: 10.1111/php.13602

ABSTRACT

The effectiveness of UVC to reduce airborne-mediated disease transmission is well established. However, conventional germicidal UVC (~254 nm) cannot be used directly in occupied spaces because of the potential for damage to the skin and eye. A recently studied alternative with the potential to be used directly in occupied spaces is far UVC (200–235 nm, typically 222 nm), as it cannot penetrate to the key living cells in the epidermis. Optimal far-UVC use is hampered by limited knowledge of the precise wavelength dependence of UVC-induced DNA damage, and thus we have used a monochromatic UVC exposure system to assess wavelength-dependent DNA damage in a realistic 3-D human skin model. We exposed a 3-D human skin model to mono-wavelength UVC exposures of 100 mJ/cm², at UVC wavelengths from 215 to 255 nm (5 nm steps). At each wavelength, we measured yields of DNA-damaged keratinocytes, and their distribution within the layers of the epidermis. No increase in DNA damage was observed in the epidermis at wavelengths from 215 to 235 nm, but at higher wavelengths (240–255 nm) significant levels of DNA damage was observed. These results support use of far-UVC radiation to safely reduce the risk of airborne disease transmission in occupied locations.

INTRODUCTION

Ultraviolet (UV) radiation encompasses wavelengths from 100 nm to 400 nm, and is further categorized into UVC (100–280 nm), UVB (280–315 nm) and UVA (315–400 nm). The effectiveness of UVC radiation to inactivate or kill microbes in the air, on surfaces or within liquids is well established (1). Epidemiological studies by Wells *et al.* in the 1930s and 1940s demonstrated the ability of UVC installations to effectively reduce the transmission of airborne diseases (2), and upper-room ultraviolet germicidal irradiation remains an effective technology which is in use internationally (3).

However, use of conventional germicidal UVC (254 nm) fixtures is limited to exposing unoccupied spaces, such as the upper-room air volume, because of the potential health hazards associated with direct exposure to this wavelength to the skin or eye, respectively, through erythema or photokeratitis (4,5).

A recent alternative to 254 nm conventional germicidal UVC is far UVC (wavelength range from 200 to 235 nm, typically used at 222 nm). Far UVC is designed to be used directly in occupied indoor locations, with good evidence published both for efficacy to inactivate airborne pathogens including influenza and coronavirus (6–15), and safety for human exposure (16–20). Far-UVC safety is premised on the fact that, because its effective range in biological material is much shorter than for conventional (254 nm wavelength) germicidal UVC (16,21–23), far-UVC incident on the skin is absorbed primarily in the superficial stratum corneum (see Fig. 1, containing only dead cells) and to a much lesser extent in the adjacent stratum granulosum (granular layer, see Fig. 1, containing dead or dying cells moving to the stratum corneum). Far-UVC light is not expected (16,21) to penetrate to the deeper stratum spinosum (spinous layer, see Fig. 1) or to the still deeper stratum basale (basal cell layer, see Fig. 1) of the epidermis, where DNA damage can result in long-term sequelae including carcinogenesis (24,25). Similar considerations apply for the eye with regard to the tear layer and the superficial cells of the cornea. In term of efficacy, however, because of the small size of viral and bacterial pathogens, far UVC can penetrate and inactivate these pathogens, typically with similar or improved efficacy compared with conventional (254 nm) germicidal UVC light (26).

While there is considerable evidence for far-UVC safety in skin and eyes (7,16,18–20,22,27–31), there have been no direct systematic measurements of DNA damage in skin as a function of wavelength that encompasses the far-UVC and conventional germicidal UVC wavelengths. This is important both from the perspective of directly validating the far-UVC concept, but also because in addition to the primary emission (*e.g.* from a KrCl* excimer lamp at 222 nm) all far-UVC light sources also emit small fluences of higher-wavelength UVC. These associated higher-wavelength UVC emissions have been shown to result in DNA damage (17), and thus most far-UVC light sources use filters to remove them. Understanding the wavelength dependence of DNA damage will allow more efficient safe filters to be designed.

Our final rationale for this study is to contribute toward improved recommendations of the UVC action spectrum and

*Corresponding author email: dw2600@cumc.columbia.edu (David Welch)
© 2022 The Authors. *Photochemistry and Photobiology* published by Wiley Periodicals LLC on behalf of American Society for Photobiology.
This is an open access article under the terms of the [Creative Commons Attribution-NonCommercial](https://creativecommons.org/licenses/by-nc/4.0/) License, which permits use, distribution and reproduction in any medium, provided the original work is properly cited and is not used for commercial purposes.

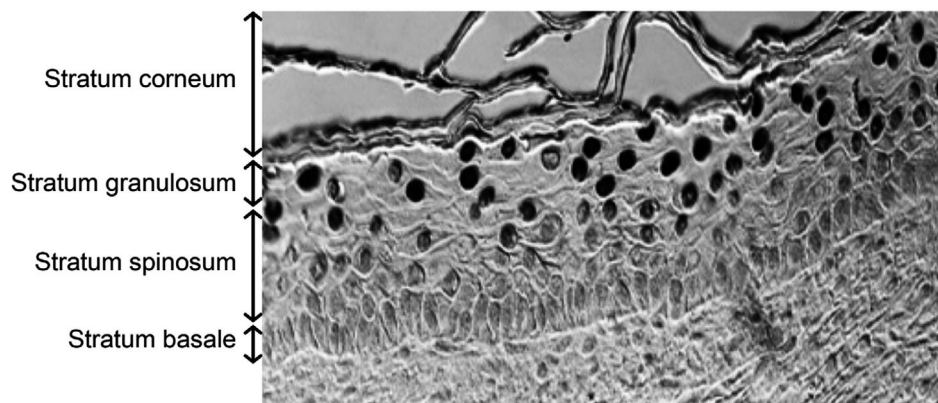


Figure 1. Representative image of the different layers of the epidermis in the 3-D human skin model, in this case exposed to 250 nm wavelength UVC. Cells with CPD DNA photodamage appear as dark-stained nuclei.

associated exposure limits by the American Conference of Governmental Industrial Hygienists (ACGIH) and the International Commission on Non-Ionizing Radiation Protection (ICNIRP), the agencies which provide regulatory recommendations with regard to UV threshold limit values or exposure limits.

In this study, we used a monochromatic exposure system designed for narrow bandwidth UVC exposures, with which we irradiated realistic 3-D models of human skin which recapitulates the key components of human skin. Using this system, we assessed the wavelength dependence of DNA photodamage measured in the whole epidermis and within the different epidermal layers.

MATERIALS AND METHODS

Monochromatic wavelength UVC exposure system. An optical system was assembled to enable monochromatic UVC exposures to 3-D models of human skin tissue. An EQ-77 Laser-Driven Light Source (Energetiq Technology, Inc., Wilmington, MA) provided a high brightness broadband output across the wavelength range of 170–2500 nm. A pair of off-axis parabolic mirrors focused the EQ-77 output into a Cornerstone 260 1/4 m monochromator (CS260-RG-2-FH-A, Newport, Irvine, CA). The monochromator was equipped with a 1201.6 g/mm plane blazed holographic reflection grating (#53*-200H with master no. 5482; 250 nm nominal blaze wavelength, Newport) to maximize optical throughput in the UVC. Fixed slits with a slit size of 600 μm (77216, Newport) were used for all experiments. The output of the monochromator was reflected downward using an off-axis replicated parabolic mirror with an aluminum coating (50329AL, Newport) to permit the exposure of samples from above. A system warm-up time of 30 min was allowed for all experiments.

UVC characterization and dosimetry. The monochromator spectral output was characterized using a BTS-2048UV Spectroradiometer (Gigahertz-Optik, Inc., Amesbury, MA). With a 600 μm slit width and the 1201.6 g/mm grating, the resolution of the monochromator was 1.9 nm. The measured full width at half maximum was between 2.0 nm and 2.2 nm for all peak wavelengths used in this study. The monochromatic spectral output for wavelengths between 215 nm and 255 nm is shown in Fig. 2 with both a log (panel A) and linear Y-axis (panel B). The throughput of the system was measured using an 843-R optical power meter (Newport) with a recently calibrated 818-UV/DB silicon detector (Newport). The detector was calibrated within the 3 months prior to the experiments. The total optical power output was measured for each wavelength examined in this work, and these data are plotted in Fig. 3. The irradiance at the target surface was determined by dividing the optical power by the beam area at the exposure plane. The beam area was characterized by using a piece of ultraviolet-sensitive film (OrthoChromic Film OC-1, Orthochrome Inc., Hillsborough, NJ) (32). The film was placed at the exposure plane and irradiated to cause a color

change illustrating the total exposure area. This area was approximately an 8 mm \times 10 mm ellipse, with an area of 62.8 mm². Film was also used to verify if the beam was fully within the detector area when measuring optical power immediately following the off-axis parabolic mirror; the beam was approximately an 8 mm \times 9 mm ellipse, so it was within the 10-mm-diameter detector area. The irradiance for each peak wavelength is also plotted on Fig. 3. The total exposure time for a given wavelength was determined by dividing the desired radiant exposure dose by the irradiance. Based on measurement uncertainties for the dimensions of the elliptical exposure area to be within ± 0.5 mm and the uncertainty of the optical power sensor of $\pm 4.2\%$ for 200–219 nm and $\pm 2.6\%$ for 220–349 nm, the total uncertainty of the irradiance values is estimated to be approximately $\pm 10\%$.

Measurement of UVC-induced CPD epidermal lesions in a 3-D human skin model. We used the 3-D human skin model EpiDerm-FT (MatTek Corp., Ashland, MA), which is derived from single adult donors. EpiDerm-FT is a full-skin thickness construct that recapitulates the key components of human skin, consisting of 8–12 cell layers of normal human epidermal keratinocytes and dermal fibroblasts that form basal, spinous, granular and cornified layers analogous to those found *in vivo* (33).

The tissues were exposed to a radiant exposure dose of 100 mJ/cm² using narrow bandwidth exposures centered at wavelength of 215, 220, 225, 230, 235, 240, 245, 250 or 255 nm. Experimental controls were unexposed 3-D tissues. Both the sham (controls) and exposed tissues were fixed 15 min after exposure. Two tissues were exposed at each of the examined wavelengths, and we measured the percentage of the most abundant premutagenic DNA photoproduct, cyclobutane pyrimidine dimers (CPD) (34), in epidermal keratinocytes, analyzing multiple fields within each tissue. The CPDs were detected using a standard immunohistochemical method previously described (35).

For each tissue, multiple randomly selected fields of view were analyzed across the tissues to determine the CPD incidence in the different strata of the epidermis (stratum granulosum, stratum spinosum and stratum basale, see Fig. 1), as well as averaged over the entire epidermis. CPD yields represent the average \pm standard deviation of keratinocytes exhibiting dimers divided by the total number of cells measured in a randomly selected fields of view. A typical field of view is shown in Fig. 1, and the total number of cells was determined by counting the number of nuclei positive for 4',6-diamidino-2-phenylindole (DAPI) using the coverslip mounting medium with DAPI (Vectashield, Burlingame, CA). Similarly, the percentage of CPD-positive keratinocytes in each layer of the epidermis was obtained by dividing the number of positive cells in that layer by the total number of cells counted in that specific layer. Uncertainties (95% and 99% confidence intervals) for the percentage of CPD-positive cells were estimated for each sample based on Agresti-Coull (adjusted Wald) confidence interval analysis (36).

RESULTS AND DISCUSSION

We irradiated the 3-D skin model with narrow bandwidth UVC exposures in order to examine changes in DNA damage biological effects associated with small changes in wavelength. With a

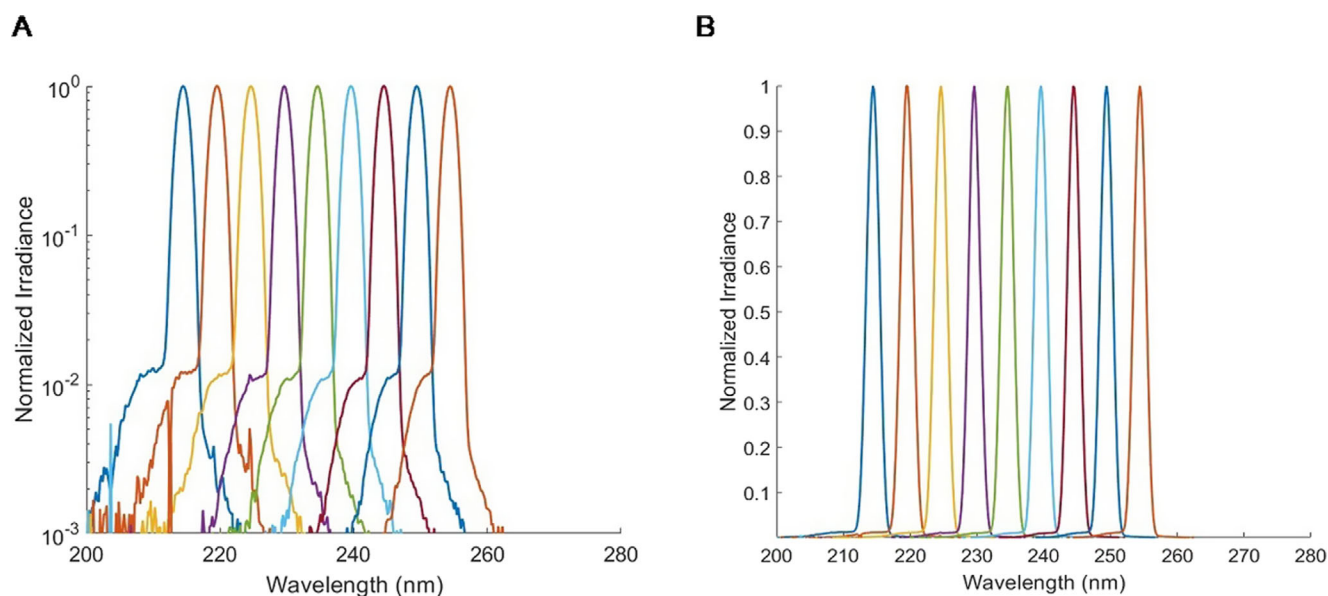


Figure 2. Spectral output of the monochromator for wavelengths tested plotted on a (A) log and (B) linear scale. The FWHM for each peak wavelength was between 2.0 nm and 2.2 nm.

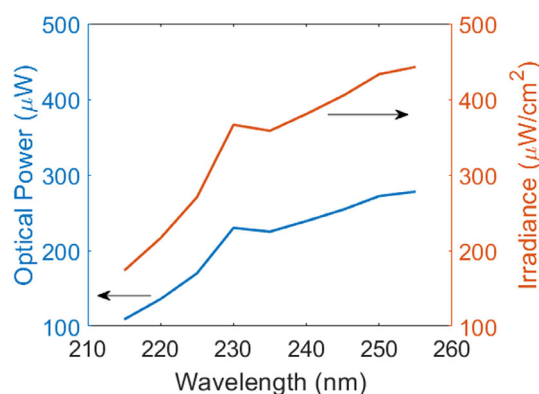


Figure 3. Monochromator optical throughput and irradiance. The total optical power was distributed over an ellipse with an area of 62.8 mm².

full width half maximum between 2.0 nm and 2.2 nm for all peak wavelengths used in this study, we exposed multiple 3-D models of normal human skin to 100 mJ/cm² of narrow bandwidth UVC at nine different wavelengths from 215 nm to 255 nm (215, 220, 225, 230, 235, 240, 245, 250 and 255 nm). The exposure of 100 mJ/cm² was chosen to be somewhat larger than the 2021 Threshold Limit Value/Exposure Limit for 222 nm of 23 mJ/cm² for an 8 h exposure.

After irradiation, sample preparation and staining, we analyzed multiple fields throughout the epidermis for CPD lesions, at the superficial granular layer (stratum granulosum), at intermediate depths (stratum spinosum) and at the basal cell layer (stratum basale).

At the five far-UVC wavelengths that we studied (215, 220, 225, 230 and 235 nm), we analyzed a total of 76 fields throughout the epidermis, with an average of 95 ± 15 keratinocyte cells per field. The results are summarized in Fig. 4A. Based on Agresti–Coull (adjusted Wald) confidence interval analysis (36), in none of the 76 epidermal fields in the far-UVC-exposed samples did we observe a statistically significant increase in CPD photolesions relative to zero exposure controls.

At the four higher UVC wavelengths that we studied (240, 245, 250 and 255 nm), we analyzed a total of 40 fields throughout the epidermis, with an average of 109 ± 21 keratinocyte cells analyzed per field. The results are summarized in Fig. 4A, and in contrast to the far-UVC results at 215–235 nm, in every 1 of the 40 epidermal fields observed after 240–255 nm exposure, a statistically significant increase in CPD photolesions relative to controls was observed, again based on Agresti–Coull confidence interval analysis.

Figure 4B shows the same CPD data but broken down into the three epidermal strata (see Fig. 1), the stratum granulosum, the stratum spinosum and the stratum basale. As shown in Fig. 4B, in the far-UVC wavelength range (215–235 nm), no CPD lesions were observed in either the stratum spinosum or the stratum basale, but a significant increase in CPDs was observed in the superficial stratum granulosum. By contrast, at the higher UVC wavelengths (240–255 nm), significant increases in CPDs vs. controls were observed in all layers, except in the basal layer at 240 nm.

The very low yields of DNA damage between 215 and 235 nm are expected due to the very high protein absorption coefficients in this wavelength range (21,37,38), as is the increase in DNA damage at 240–255 nm due to the correspondingly lower absorption coefficients (21,37,38). The significant variations in DNA damage observed from 240 to 255 nm can be attributed to the existence of sharp local maxima and minima in UV absorbance of different proteins in this higher-wavelength range (39,40).

To put these stratum-specific results into context (and see Fig. 1), the stratum basale is the deepest layer of the epidermis, where basal cells, including melanocytes, are constantly dividing and migrating upwards; above the stratum basale is the stratum spinosum which contains squamous cells and provides the skin's structural integrity; and above the stratum spinosum is the stratum granulosum which contains dead or dying cells whose nuclei and other organelles are disintegrating as the cells move up into the stratum corneum (41). Thus, from a long-term safety

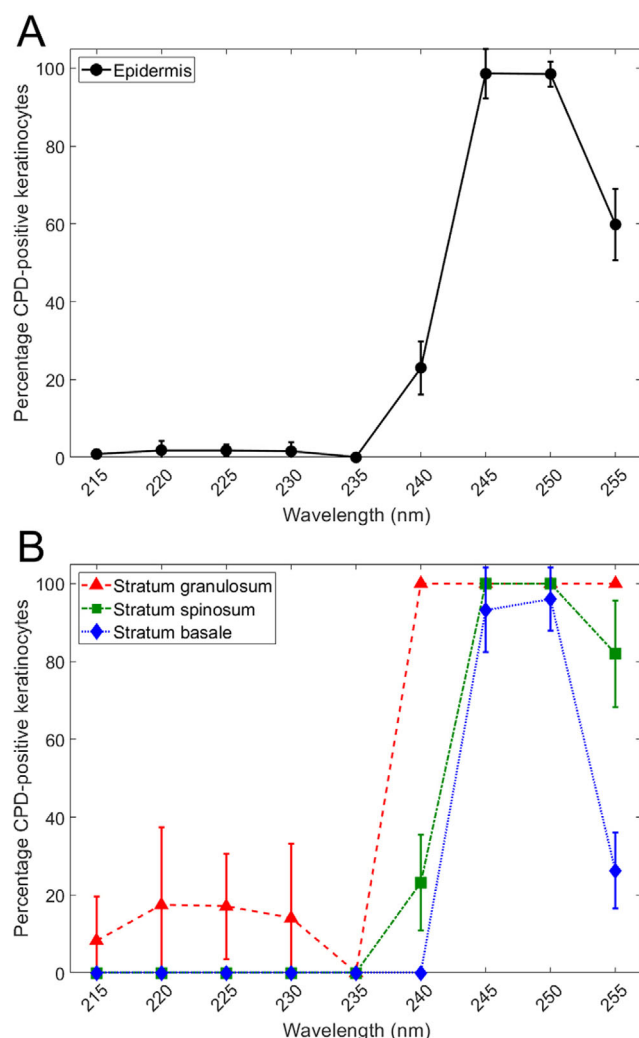


Figure 4. Percentage of DNA photodamage induced by 100 mJ/cm² in the UVC wavelength range. Percentage of the total keratinocytes positive for CPD counted in (A) the whole epidermis and (B) each layer (see Fig. 1) of the epidermis. Error bars indicate standard deviations.

perspective, the concern relates to DNA damage to cells in the stratum basale and stratum spinosum, which contain living basal cells, melanocytes and squamous cells (24,25,42). DNA damage to cells in the stratum granulosum or, of course, the stratum corneum is of much less concern, as these contain dead or dying cells.

We may conclude from these results that, at UVC exposures of 100 mJ/cm², far UVC (215–235 nm) did not produce a significant increase in DNA photodamage averaged over the epithelium, and did not produce any DNA photodamage in the relevant epithelial layers, namely the stratum basale and the stratum spinosum. By contrast, exposure to the higher UVC wavelengths studied (240–255 nm) does produce significant increases in DNA photodamage in the epithelium, and at each of the epithelial layers studied.

The results of Yamano *et al.* (43), in which mice skin was exposed to far-UVC radiation, provide a comparison for the findings of this work. In that study, some weakly stained CPD-positive cells were observed within the basal layer following exposure to 200 mJ/cm² of 235 nm radiation (4 nm full width at half maximum). This is in contrast to the present study which

did not reveal any CPDs in the basal layer with 100 mJ/cm² of 235 nm radiation. Probable explanations for this discrepancy include the lower dose used in this study (100 mJ/cm²) and the difference in epidermal thickness between the human skin model used here and the thinner epidermis in the mouse model (44,45). Also, the difference in bandwidth between the two exposures is important, with the longer wavelengths in the wider 4 nm full width at half maximum used by Yamano *et al.* possibly providing a significant amount of the observed DNA photodamage from that work.

As well as providing support for the basic concept of far-UVC safety, the results shown here should allow for optimized design of UVC filters designed to reduce the higher-wavelength UV spectral impurities that are typically associated with far-UVC light sources (17). In addition, these results should contribute toward improved recommendations of UVC action spectra; these results suggest that, at least for skin, the 2021 ACGIH Threshold Limit Values for far UVC may be overprotective.

In conclusion, these results provide quantitative wavelength-specific data supporting the safe use of far-UVC in occupied public settings. The data were generated using a realistic 3-D human skin model exposed to UVC exposures of 100 mJ/cm², somewhat higher than the 2021 ACGIH Threshold Limit Value/Exposure Limit for 222 nm radiation of 23 mJ/cm²/8 h exposure. At this exposure, no photodamage was observed in the key epidermal layers of the stratum basale and the stratum spinosum—the locations of epidermal basal cells, melanocytes and squamous cells—at the far-UVC wavelengths of 215, 220, 225, 230 and 235 nm, in contrast to higher UVC wavelengths (240, 245, 250 and 255 nm) where significant levels of photodamage were observed.

Acknowledgements—This work funded in part under an AFWERX SBIR with the 189th Airlift Wing, Arkansas Air National Guard and Far UV Technologies, as well as from the Shostack Foundation and LumenLabs. We thank Dr. Gerhard Randers-Pehrson for his conceptual insights. We are grateful to the Ultraviolet Radiation Group of the Sensor Science Division in the NIST Physical Measurement Laboratory for assistance with the monochromator system design.

DATA AVAILABILITY STATEMENT

Data are available on the Open Science Framework (OSF) repository: <https://osf.io/aj7yc/>

REFERENCES

1. Kowalski, W. J. (2009) *Ultraviolet Germicidal Irradiation Handbook: UVGI for Air and Surface Disinfection*. Springer, New York.
2. Wells, W., M. Wells and T. Wilder (1942) The environmental control of epidemic contagion. I. An epidemiologic study of radiant disinfection of air in day schools. *Am. J. Hyg.* **35**, 97–121.
3. Nardell, E., R. Vincent and D. H. Sliney (2013) Upper-room ultraviolet germicidal irradiation (UVGI) for air disinfection: a symposium in print. *Photochem. Photobiol.* **89**(4), 764–769.
4. 2021 Threshold Limit Values and Biological Exposure Indices. 2021: American Conference of Governmental Industrial Hygienists.
5. The International Commission on Non-Ionizing Radiation Protection (2004) Guidelines on limits of exposure to ultraviolet radiation of wavelengths between 180 nm and 400 nm (incoherent optical radiation). *Health Phys.* **87**(2), 171–186.
6. Buchan, A. G., L. Yang and K. D. Atkinson (2020) Predicting airborne coronavirus inactivation by far-UVC in populated rooms using a high-fidelity coupled radiation-CFD model. *Sci. Rep.* **10**(1), 19659.

7. Buonanno, M., B. Ponnaiya, D. Welch, M. Stanislauskas, G. Randers-Pehrson, L. Smilenov, F. D. Lowy, D. M. Owens and D. J. Brenner (2017) Germicidal efficacy and mammalian skin safety of 222-nm UV light. *Radiat. Res.* **187**(4), 483–491.
8. Buonanno, M., D. Welch, I. Shuryak and D. J. Brenner (2020) Far-UVC light (222 nm) efficiently and safely inactivates airborne human coronaviruses. *Sci. Rep.* **10**(1), 10285.
9. Eadie, E., W. Hiwar, L. Fletcher, E. Tidswell, P. O'Mahoney, M. Buonanno, D. Welch, C. S. Adamson, D. J. Brenner, C. Noakes and K. Wood. Far-UVC efficiently inactivates an airborne pathogen in a room-sized chamber. *Sci. Rep.* www.researchsquare.com/article/rs-908156/v1
10. Glaab, J., N. Lobo-Ploch, H. K. Cho, T. Filler, H. Gundlach, M. Guttman, S. Hagedorn, S. B. Lohan, F. Mehnke and J. Schleusener (2021) Skin tolerant inactivation of multiresistant pathogens using far-UVC LEDs. *Sci. Rep.* **11**(1), 1–11.
11. Goh, J. C., D. Fisher, E. C. H. Hing, L. Hanjing, Y. Y. Lin, J. Lim, O. W. Chen and L. T. Chye (2021) Disinfection capabilities of a 222 nm wavelength ultraviolet lighting device: a pilot study. *J. Wound Care* **30**(2), 96–104.
12. Kitagawa, H., Y. Kaiki, K. Tadera, T. Nomura, K. Omori, N. Shigemoto, S. Takahashi and H. Ohge (2021) Pilot study on the decontamination efficacy of an installed 222-nm ultraviolet disinfection device (Care222™), with a motion sensor, in a shared bathroom. *Photodiagn. Photodyn. Ther.* **34**, 102334.
13. Kitagawa, H., T. Nomura, T. Nazmul, R. Kawano, K. Omori, N. Shigemoto, T. Sakaguchi and H. Ohge (2021) Effect of intermittent irradiation and fluence-response of 222 nm ultraviolet light on SARS-CoV-2 contamination. *Photodiagn. Photodyn. Ther.* **33**, 102184.
14. Kitagawa, H., T. Nomura, T. Nazmul, K. Omori, N. Shigemoto, T. Sakaguchi and H. Ohge (2021) Effectiveness of 222-nm ultraviolet light on disinfecting SARS-CoV-2 surface contamination. *Am. J. Infect. Control* **49**(3), 299–301.
15. Welch, D., M. Buonanno, V. Grilj, I. Shuryak, C. Crickmore, A. W. Bigelow, G. Randers-Pehrson, G. W. Johnson and D. J. Brenner (2018) Far-UVC light: a new tool to control the spread of airborne-mediated microbial diseases. *Sci. Rep.* **8**(1), 2752.
16. Barnard, I. R. M., E. Eadie and K. Wood (2020) Further evidence that far-UVC for disinfection is unlikely to cause erythema or pre-mutagenic DNA lesions in skin. *Photodermatol. Photoimmunol. Photomed.* **36**(6), 476–477.
17. Buonanno, M., D. Welch and D. J. Brenner (2021) Exposure of human skin models to KrCl excimer lamps: the impact of optical filtering†. *Photochem. Photobiol.* **97**(3), 517–523.
18. Eadie, E., I. M. Barnard, S. H. Ibbotson and K. Wood (2021) Extreme exposure to filtered far-UVC: a case study. *Photochem. Photobiol.* **97**(3), 527–531.
19. Fukui, T., T. Niikura, T. Oda, Y. Kumabe, H. Ohashi, M. Sasaki, T. Igarashi, M. Kunisada, N. Yamano, K. Oe, T. Matsumoto, T. Matsushita, S. Hayashi, C. Nishigori and R. Kuroda (2020) Exploratory clinical trial on the safety and bactericidal effect of 222-nm ultraviolet C irradiation in healthy humans. *PLoS One* **15**(8), e0235948.
20. Hickerson, R., M. Conneely, S. Hirata Tsutsumi, K. Wood, D. Jackson, S. Ibbotson and E. Eadie (2021) Minimal, superficial DNA damage in human skin from filtered far-ultraviolet C. *Br. J. Dermatol.* **184**(6), 1197–1199.
21. Finlayson, L., I. R. M. Barnard, L. McMillan, S. H. Ibbotson, C. T. A. Brown, E. Eadie and K. Wood (2021) Depth Penetration of Light into Skin as a Function of Wavelength from 200 to 1000 nm. *Photochem. Photobiol.* [Doi:10.1111/php.13550](https://doi.org/10.1111/php.13550)
22. Cadet, J. (2020) Harmless effects of sterilizing 222-nm far-UV radiation on mouse skin and eye tissues. *Photochem. Photobiol.* **96**(4), 949–950.
23. Cesarini, J.-P., C. Cole and F. de Grujil (2010) UV-C photocarcinogenesis risks from germicidal lamps. *Int. Commission Illumination* **187**, 1–14.
24. Forbes, P. D., C. A. Cole and F. de Grujil (2021) Origins and evolution of photocarcinogenesis action spectra, including germicidal UVC(dagger). *Photochem. Photobiol.* **97**(3), 477–484.
25. de Grujil, F. R. and C. P. Tensen (2018) Pathogenesis of skin carcinomas and a stem cell as focal origin. *Front. Med.* **5**, 165.
26. Ma, B., P. M. Gundy, C. P. Gerba, M. D. Sobsey and K. G. Linden (2021) UV inactivation of SARS-CoV-2 across the UVC spectrum: KrCl* excimer, mercury-vapor, and light-emitting-diode (LED) sources. *Appl. Environ. Microbiol.* **87**(22), e0153221.
27. Eadie, E., P. O'Mahoney, L. Finlayson, I. R. M. Barnard, S. H. Ibbotson and K. Wood (2021) Computer modeling indicates dramatically less DNA damage from Far-UVC Krypton chloride lamps (222 nm) than from sunlight exposure. *Photochem. Photobiol.* **97**(5), 1150–1154.
28. Hanamura, N., H. Ohashi, Y. Morimoto, T. Igarashi and Y. Tabata (2020) Viability evaluation of layered cell sheets after ultraviolet light irradiation of 222 nm. *Regen. Ther.* **14**, 344–351.
29. Kaidzu, S., K. Sugihara, M. Sasaki, A. Nishiaki, T. Igarashi and M. Tanito (2019) Evaluation of acute corneal damage induced by 222-nm and 254-nm ultraviolet light in Sprague-Dawley rats. *Free Radical Res.* **53**(6), 611–617.
30. Kaidzu, S., K. Sugihara, M. Sasaki, A. Nishiaki, H. Ohashi, T. Igarashi and M. Tanito (2021) Re-evaluation of rat corneal damage by short-wavelength UV revealed extremely less hazardous property of Far-UV-C. *Photochem. Photobiol.* **97**(3), 505.
31. Yamano, N., M. Kunisada, S. Kaidzu, K. Sugihara, A. Nishiaki-Sawada, H. Ohashi, A. Yoshioka, T. Igarashi, A. Ohira, M. Tanito and C. Nishigori (2020) Long-term effects of 222-nm ultraviolet radiation C sterilizing lamps on mice susceptible to ultraviolet radiation. *Photochem. Photobiol.* **96**(4), 853–862.
32. Welch, D. and D. J. Brenner (2021) Improved ultraviolet radiation film dosimetry using OrthoChromic OC-1 Film(dagger). *Photochem. Photobiol.* **97**(3), 498–504.
33. Kubilus, J., P. J. Hayden, S. Ayejunie, S. D. Lamore, C. Servattalab, K. L. Bellavance, J. E. Sheasgreen and M. Klausner (2004) Full Thickness EpiDerm: a dermal-epidermal skin model to study epithelial-mesenchymal interactions. *Altern. Lab. Anim.* **32**(Suppl 1A), 75–82.
34. Pfeifer, G. P. and A. Besaratinia (2012) UV wavelength-dependent DNA damage and human non-melanoma and melanoma skin cancer. *Photochem. Photobiol. Sci.* **11**(1), 90–97.
35. Buonanno, M., M. Stanislauskas, B. Ponnaiya, A. W. Bigelow, G. Randers-Pehrson, Y. Xu, I. Shuryak, L. Smilenov, D. M. Owens and D. J. Brenner (2016) 207-nm UV light-A promising tool for safe low-cost reduction of surgical site infections. II: in-vivo safety studies. *PLoS One* **11**(6), e0138418.
36. Agresti, A. and B. A. Coull (1998) Approximate is better than “exact” for interval estimation of binomial proportions. *Am. Stat.* **52**(2), 119–126.
37. Buonanno, M., G. Randers-Pehrson, A. W. Bigelow, S. Trivedi, F. D. Lowy, H. M. Spotnitz, S. M. Hammer and D. J. Brenner (2013) 207-nm UV light - A promising tool for safe low-cost reduction of surgical site infections. I: in vitro studies. *PLoS One* **8**(10), e76968.
38. Kreuz, S., S. Schwedler, B. Tautkus, G. A. Cumme and A. Horn (2003) UV measurements in microplates suitable for high-throughput protein determination. *Anal. Biochem.* **313**(2), 208–215.
39. Lakowicz, J. R. (2013) *Principles of fluorescence spectroscopy*. Boston, MA: Springer Science & Business Media.
40. Tozar, T., I. R. Andrei, R. Costin, R. Pirvulescu and M. L. Pasco (2018) Case series about ex vivo identification of squamous cell carcinomas by laser-induced autofluorescence and Fourier transform infrared spectroscopy. *Lasers Med. Sci.* **33**(4), 861–869.
41. Barbieri, J. S., K. Wanat and J. Seykora (2014) Skin: Basic Structure and Function. In *Pathobiology of Human Disease* (Edited by L. M. McManus and R. N. Mitchell), pp. 1134–1144. Academic Press, San Diego.
42. Black, H. S., F. R. deGrujil, P. D. Forbes, J. E. Cleaver, H. N. Ananthaswamy, E. C. deFabo, S. E. Ullrich and R. M. Tyrrell (1997) Photocarcinogenesis: an overview. *J. Photochem. Photobiol. B* **40**(1), 29–47.
43. Yamano, N., M. Kunisada, A. Nishiaki-Sawada, H. Ohashi, T. Igarashi and C. Nishigori (2021) Evaluation of acute reactions on mouse skin irradiated with 222 and 235 nm UV-C. *Photochem. Photobiol.* **97**(4), 770–777.
44. Ponc, M., E. Boelsma, S. Gibbs and M. Mommaas (2002) Characterization of reconstructed skin models. *Skin Pharmacol. Physiol.* **15**(Suppl. 1), 4–17.
45. Wei, J. C. J., G. A. Edwards, D. J. Martin, H. Huang, M. L. Crichton and M. A. F. Kendall (2017) Allometric scaling of skin thickness, elasticity, viscoelasticity to mass for micro-medical device translation: from mice, rats, rabbits, pigs to humans. *Sci. Rep.* **7**(1), 15885.